Journal of Photochemistry and Photobiology A: Chemistry 202 (2009) 191–195

Contents lists available at ScienceDirect

Journal of Photochemistry and Photobiology A: Chemistry

journal homepage: www.elsevier.com/locate/jphotochem

Negative shift of chlorophyll *a* oxidation potential by aggregation in acetonitrile/ionic liquid mixed solvents

Yoshinori Kuroiwa, Yuki Kato, Tadashi Watanabe*

Institute of Industrial Science, The University of Tokyo, 4-6-1 Komaba, Meguro-ku, Tokyo 153-8505, Japan

ARTICLE INFO

Article history:
Received 7 August 2008
Received in revised form 29 October 2008
Accepted 3 December 2008
Available online 11 December 2008

Keywords:
Photosynthesis
Chlorophyll
Dimerization
Aggregation

ABSTRACT

Spectroscopic and electrochemical properties of chlorophyll (Chl) *a* aggregates in mixed solvents of acetonitrile and an ionic liquid, 1-ethyl-3-methylimidazolium tetrafluoroborate ($EMIBF_4$), were examined. The red-shifted absorption peak of the Q_y band due to Chl *a* aggregation as well as the log[Chl *a* aggregate] against log[Chl *a* monomer] plot suggested the formation of low-order aggregates such as a dimer. Square wave voltammetry revealed that the first oxidation potential of the Chl *a* aggregate in the AN/$EMIBF_4$ mixed solvents is shifted negatively by 130 mV from that of Chl *a* monomer. In comparison with the redox potential of Chl *a* in vivo, a tuning mechanism of the redox potentials for photosynthetic species due to dimerization/aggregation is discussed.

1. Introduction

Chlorophylls capture solar energy and convert it into chemical energy in oxygenic photosynthesis. Among chlorophylls, chlorophyll (Chl) *a* plays key roles in charge separation and electron transport within reaction centers of photosystems [1]. Recent X-ray crystallographic analyses of photosystem I revealed that Chl *a* and its $C13^2$ epimer, Chl *a*′, form a heterodimer called P700 [2,3], playing as the primary electron donor. Dimerization of Chls yields red-shifted absorption, which enables P700 to receive effectively the excitation energy from peripheral pigments. Further, dimerization shifts the electron energy level to a reductive direction, i.e., enhances a reductive power, leading finally to reduction of $NADP^+$ to NADPH. The first oxidation potential of P700 (the $P700/P700^+$ redox potential) in vivo is around +450 mV *vs.* SHE [4,5], while the potential of Chl *a*/Chl a^+ in vitro is around +800 mV *vs.* SHE (see a review [6], from +0.76 to +0.94 V depending on the environment), indicating that the reductive power of P700 is enhanced by over 300 mV.

These phenomena have triggered many works on the physicochemical properties of dimerized and/or aggregated Chl *a* molecules in vitro [7–14] to characterize Chl *a* aggregates and mimic photosynthetic architectures. To promote aggregation of Chl *a* in vitro, mixtures of organic solvents and water have generally been used as a medium in many works [7–11]. Adding a small amount of water into organic solvent-based solutions containing Chl *a* induces aggregation, which is reflected by red-shifted absorption of Chl *a*. In addition to UV–vis absorption and fluorescence measurements, studies using circular dichroism (CD) [10], resonance Raman [12], infrared [13], NMR [14], ESR [15], transmission electron microscopy (TEM) [11] etc. have been done for spectroscopic and structural characterization of Chl *a* aggregates. However, few studies were reported on the electrochemical properties of Chl *a* aggregates. Agostiano et al. [8] investigated electrochemical behavior of Chl *a* aggregates in mixtures of an organic solvent and water, and revealed the formation of different solvated species of Chl *a* by polarography with a hanging mercury drop electrode. They distinguished such species as a dihydrate dimer, a monohydrate dimer and oligomers of Chl *a* based on the Chl *a*/Chl a^- redox potentials, where the potential shifted negatively by ca. 100 mV upon aggregation; however, no direct information was acquired for the shift of the oxidation (Chl *a*/Chl a^+) potential. The nature of the mercury electrode prevents measurements in the anodic potential region [16].

The high polarity and high electrochemical stability (wide potential window) of ionic liquids are useful for studying the Chl *a*/Chl a^+ redox reaction as well as inducing Chl *a* aggregation. Ionic liquids are a new class of solvents and differ from conventional molecular solvents in respect to thermal stability, low volatility, solubility and acidity/basicity as well as polarity and electrochemical stability, permitting novel uses in such fields as material synthesis, analytical chemistry, separation technology, and electrochemical devices [17]. In the present study, spectroscopic and electrochemical properties of the Chl *a* aggregates in mixed solvents of acetonitrile (AN) and an ionic liquid 1-ethyl-3-methylimidazolium tetrafluoroborate ($EMIBF_4$) were examined.

Abbreviations: Chl, chlorophyll; $EMIBF_4$, 1-ethyl-3-methylimidazolium tetrafluoroborate; AN, acetonitrile; SWV, square wave voltammetry.

* Corresponding author. Tel.: +81 3 5452 6330; fax: +81 3 5452 6331.
E-mail address: watanabe@iis.u-tokyo.ac.jp (T. Watanabe).

1010-6030/$ – see front matter © 2008 Elsevier B.V. All rights reserved.
doi:10.1016/j.jphotochem.2008.12.006

Square wave voltammetry enabled us to detect, for the first time, the negative shift of the oxidation potential of Chl *a* upon aggregation. The redox potential shift in vitro thus determined is compared with that in vivo and the difference between them is briefly discussed.

2. Materials and methods

2.1. Materials

HPLC grade hexane, methanol, 2-propanol, acetone and acetonitrile (Wako pure Chemicals, Ltd.) were used for extraction and purification of Chl *a*. Anhydrous grade acetonitrile (AN; 99.8% purity, H_2O <10 ppm, Aldrich) and 1-ethyl-3-methylimidazolium tetrafluoroborate ($EMIBF_4$; 98%, Kanto Chemical, Ltd.) were used for spectroscopy and electrochemistry. AN was dried with molecular sieves for over 24 h before use. $EMIBF_4$ was dried in a vacuum oven at 120 °C for over 24 h and kept with molecular sieves before the measurements.

2.2. Chl a preparation

Chl *a* was extracted and purified as described elsewhere [18]. Briefly, the pigments were extracted with acetone from lyophilized spinach leaves, and were subjected to column chromatography to obtain roughly purified Chl *a*. Crude Chl *a* was then purified by normal-phase HPLC (column: Senshupak, Silica-5251N) using hexane/2-propanol/methanol = 100/0.8/0.4 as eluent. Chl *a* was stored in 5 mL glass vials at −30 °C until use. Reversed-phase HPLC (column, Senshupak nucleosil 100-5C18; eluent, acetonitrile/methanol/ethanol/H_2O = 85/9/3/3) was performed to examine the degree of Chl *a* denaturation. The purity of Chl *a* was higher than 99% just before use.

2.3. Spectroscopy and electrochemistry

Spectroscopic studies on Chl *a* aggregates were done as follows. Chl *a* was homogeneously suspended in AN, and $EMIBF_4$ was added there. After stirring, the solution suspending Chl *a* was incubated for 3 h in the dark. The Chl *a* concentration was 250 μM. Visible absorption spectra of the solutions were recorded on a JASCO spectrophotometer Model UV-560. Fluorescence measurements were performed on a JASCO fluorescence spectrophotometer FP-6500 with excitation at 430 nm. Reversed-phase HPLC was performed to ensure the integrity of Chl *a* before and after the measurements.

The redox potentials of Chl *a* in the mixed solvents were measured by square wave voltammetry (SWV) [19] with an ALS Instrument electrochemical analyzer Model 620A. An electrochemical cell consisting of a gold disk working electrode (ϕ: 1.6 mm), a platinum black wire counter electrode and an Ag/AgCl reference electrode was used. The redox potential of the ferrocene–ferrocinium couple was measured to examine junction potential changes by changing the $EMIBF_4$ concentration in the mixed solvents.

3. Results and discussion

Aggregation of chlorophylls is known to yield red-shifted absorption in the Soret and Q_y band regions [7–14]. Fig. 1(a) shows the absorption spectra of Chl *a* in the AN/$EMIBF_4$ solvents at various $EMIBF_4$ concentrations. With increasing $EMIBF_4$ concentration, the absorbance peaks at both 430 nm (Soret band) and 662 nm (Q_y band) tended to diminish, while an absorption tail appeared in the longer wavelength region of the Q_y band. The difference spectra, obtained by subtracting the absorption spectra around the Q_y band from the Chl *a* monomer absorption spectrum (Fig. 1(b)), clearly show absorbance changes, decreasing at 660 nm and increasing at 685 nm. These demonstrate a decrease in the Chl *a* monomer fraction due to aggregate formation as the $EMIBF_4$ concentration was increased.

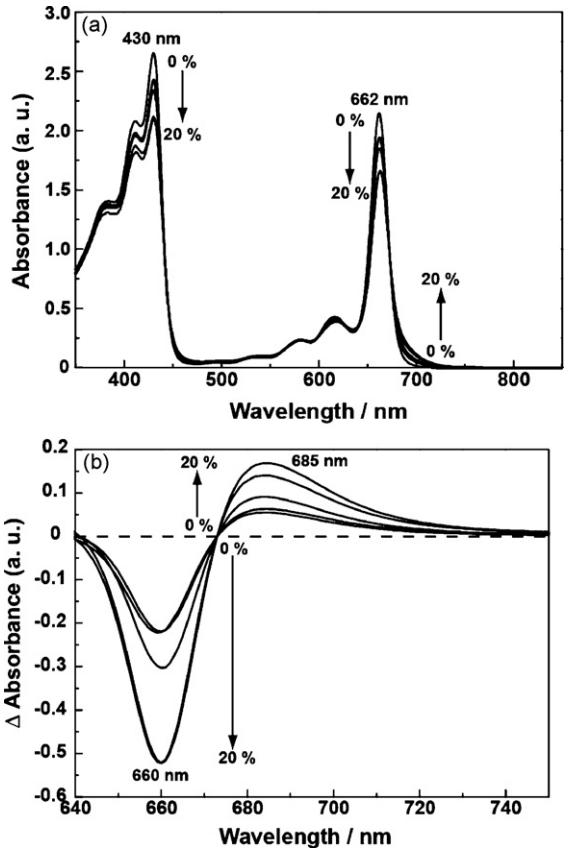

Fig. 1. (a) Absorption spectra of Chl *a* (250 μM) in acetonitrile (AN)/$EMIBF_4$ at various $EMIBF_4$ concentrations and (b) difference spectra in the Q_y band of Chl *a* absorption in AN/$EMIBF_4$.

Fig. 2 shows the fluorescence spectra of Chl *a* in the mixed solvents at a series of $EMIBF_4$ concentrations. The shape of the fluorescence spectra changed more drastically as compared with the absorption spectra, Fig. 1(a), by addition of $EMIBF_4$. Chl *a* monomer generally shows a fluorescence spectrum with a sharp peak around 670–680 nm in literature [for example [9,11,15]]; however, the fluorescence spectrum of Chl *a* in AN without $EMIBF_4$ where monomeric Chl *a* alone exists yields a weak and broad band at around 689 nm,

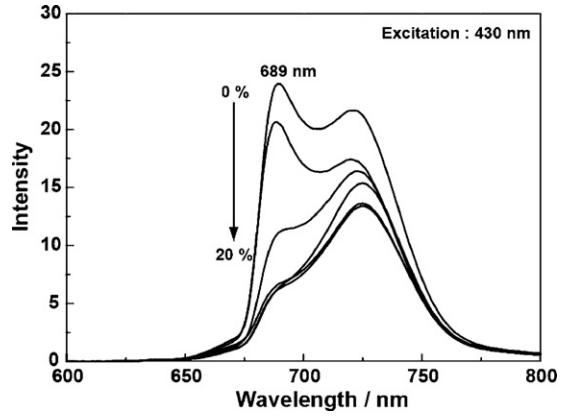

Fig. 2. Fluorescence spectra of Chl *a* (250 μM) in AN/$EMIBF_4$ at various $EMIBF_4$ concentrations.

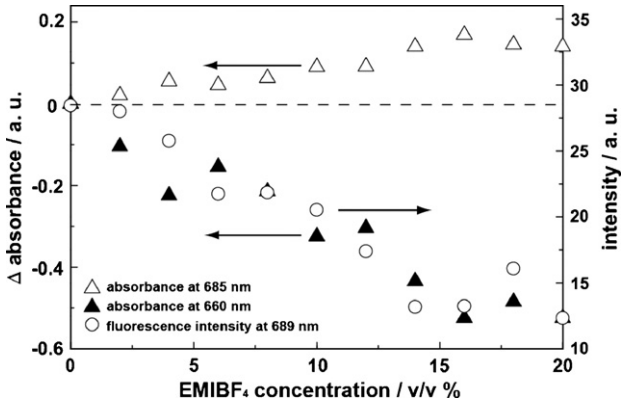

Fig. 3. Absorbances at 660 and 685 nm and fluorescence intensities at 689 nm of Chl *a* as a function of $EMIBF_4$ concentration in AN/$EMIBF_4$.

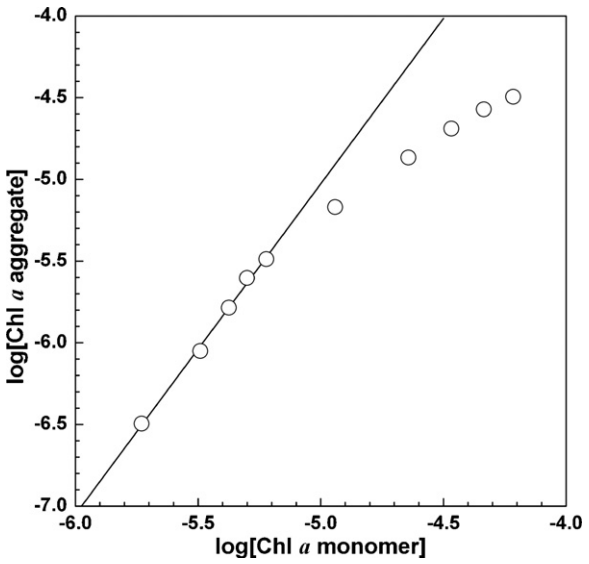

Fig. 4. Plot of log[Chl *a* aggregate] against log[Chl *a* monomer] for a series of total Chl *a* concentration (2.5–250 μM) in AN/$EMIBF_4$ = 84/16. The molar absorption coefficients of Chl *a* monomer and aggregate are 8.3×10^4 and 5.94×10^4 M^{-1} cm^{-1}, respectively, and the slope of the solid line is 2.0.

most probably due to concentration quenching because the Chl *a* concentration (250 μM) was much higher than that in the literature. Further, with increasing $EMIBF_4$ concentration, the fluorescence intensity at 689 nm tended to decay. Since the fluorescence decay suggests the increase in intermolecular interaction between Chl *a* molecules, the intensity at 689 nm reflects a change in the Chl *a* monomer fraction. Meanwhile, the 725 nm/689 nm intensity ratio increased as the concentration of $EMIBF_4$ was increased. This tendency should be induced by the formation of a Chl *a* aggregate absorbing at around 685 nm, absorbing the fluorescence from Chl *a* monomer. Therefore, the fluorescence intensity change at 689 nm also implies that Chl *a* forms aggregates in AN/$EMIBF_4$.

Reversed-phase HPLC before and after the spectroscopic measurements ensured that the above absorption/fluorescence spectral changes were not due to denaturation of Chl *a* by addition of $EMIBF_4$ into the solution.

The absorbance values at 660 and 685 nm for Chl *a* are depicted in Fig. 3 as a function of $EMIBF_4$ concentration in AN/$EMIBF_4$. The values changed roughly linearly up to 12% (v/v) of $EMIBF_4$; the absorbance at 685 nm increased at the expense of that at 660 nm. Above the $EMIBF_4$ concentration of 12% (v/v), the absorbance changes became sluggish. A similar tendency is noted also for the fluorescence intensity at 689 nm as seen in Fig. 3. When the concentration of $EMIBF_4$ was increased to a level higher than 20%, precipitation or colloid formation of Chl *a* in the solution was observed visually. Chl molecules generally form colloids in aqueous media, especially at high water concentrations, and often exhibit a heavily red-shifted absorption (from 660 nm to ca. 730–760 nm) [8,10,11], suggesting that Chl molecules in aqueous media form large oligomers. In some reports, species with a slightly (15–20 nm) red-shifted absorption were also observed and were assigned as a dimer of Chl *a* dihydrate [9,15]. Therefore, the present results suggest that the Chl *a* species absorbing at 685 nm in solutions at the $EMIBF_4$ concentration below 20% (v/v) may be such low-order aggregates as a dimer.

The plot of log[Chl *a* aggregate] against log[Chl *a* monomer] was performed to examine the order of Chl *a* aggregates based on the absorbance values in AN/$EMIBF_4$ = 84/16 for a series of Chl *a* concentration from 2.5 to 250 μM. The plot, as shown in Fig. 4, gave a straight line with a slope of 2 at lower concentrations. Although the data points deviated from the straight line at higher concentrations, this result indicates that no aggregates higher than dimers exist in the solvents.

Redox potentials of Chl *a* in the AN/$EMIBF_4$ solutions were measured by SWV. A high signal-to-noise ratio of SWV is useful especially for investigating redox couples with high molecular weights at such relatively low concentration as in the present work [19]. Fig. 5(a) shows the square wave voltammograms of Chl *a* in AN/$EMIBF_4$. Although electrochemical measurements were difficult in the Chl *a*/AN solution without $EMIBF_4$ because of the low conductivity of the solution, addition of 1% $EMIBF_4$ was sufficient to study the redox process of Chl *a*, since $EMIBF_4$ plays a role of a supporting electrolyte. Two oxidation peaks are seen in each voltammogram at +0.84 V and ca. +1.1 V (*vs.* SHE). The peak at +0.84 V is almost equal to that of Chl *a* one-electron oxidation in AN with a supporting electrolyte such as $NaClO_4$ [6] or tetrabutylammonium perchlorate (Bu_4NClO_4) [19]. The peak at +0.84 V in the present measurements is hence due to the first oxidation of Chl *a* (Chl *a*/Chl a^+), corresponding to the HOMO energy level. Similarly, the peak at ca. +1.1 V reflects most probably the second oxidation of Chl *a* (Chl a^+/Chl a^{2+}). These waves were confirmed as arising from one-electron reversible processes by cyclic voltammetry (data not shown).

In the square wave voltammogram of Chl *a* for 20% (v/v) $EMIBF_4$, where aggregation of Chl *a* is evident by visible spectroscopy (Fig. 3), a shoulder appeared in the potential range negative of the first oxidation of monomeric Chl *a*. Deconvolution of the voltammogram by a Gaussian curve fitting method was able to extract a peak, contributing to the shoulder, at +710 mV *vs.* SHE. The voltammograms of Chl *a* in AN/$EMIBF_4$ at a series of $EMIBF_4$ concentrations were then analyzed by Gaussian fitting (see the voltammogram of AN/$EMIBF_4$ = 90/10 as an example). The values of the peak current that contributed to the shoulders are summarized in Fig. 5(b) together with the absorbance at 685 nm induced by aggregation of Chl *a*. A good coincidence between the two values indicates unambiguously that the shoulders observed on the voltammograms of Chl *a* in AN/$EMIBF_4$ denote the oxidation current of a Chl *a* aggregate. Further, the sufficiently large oxidation current for the +710 mV peak strongly supports the idea that Chl *a* molecules form such a low-order aggregate as a dimer, since high-order aggregates would not yield sizeable oxidation current due to slow diffusion. The potential of aggregate oxidation was +0.71 V in all of the AN/$EMIBF_4$ solutions used here, and that for the peak of monomeric Chl *a* oxidation was +0.84 V, whereby no potential junction change was observed at a series of $EMIBF_4$ concentrations (the redox potential of ferrocene-ferrocinium couple was +0.47 V *vs.* Ag/AgCl in each solution). We thus conclude that addition of $EMIBF_4$ to AN

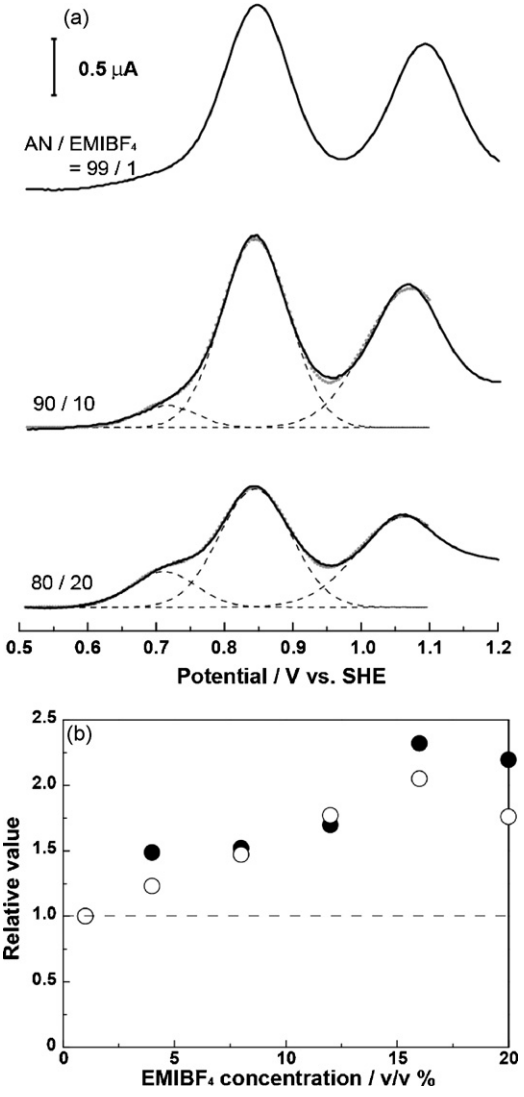

Fig. 5. (a) Square wave voltammograms of Chl *a* (250 μM) in AN/$EMIBF_4$ at three $EMIBF_4$ concentrations. Parameters for SWV: potential step = 5.0 mV, AC pulse height = 25 mV and pulse frequency = 8 Hz. The redox potential of the ferrocene–ferrocinium couple was +0.47 V *vs.* Ag/AgCl. The voltammograms for Chl *a* in AN/$EMIBF_4$ = 90/10 and 80/20 were deconvoluted by a Gaussian curve fitting method: dotted curve, best fit for experimental data; dashed curves, deconvoluted components. (b) Correlation between the oxidation current at +710 mV and the absorbance at 685 nm for Chl *a* as a function of $EMIBF_4$ concentration in AN/$EMIBF_4$.

containing Chl *a* causes it to form a low-order aggregate possessing the first oxidation potential negative of monomeric Chl *a* by 130 mV.

These results have demonstrated, for the first time, the spectroscopic and electrochemical properties of a Chl *a* aggregate, that is most probably a dimer, in mixed solvents of AN and an ionic liquid, $EMIBF_4$. SWV clearly showed that Chl *a* aggregation (or dimerization) shifts the first oxidation potential of Chl *a* to a negative direction. This result is summarized in Fig. 6. The first reduction potentials of Chl *a*/Chl a^- were estimated by assuming that the Q_y peak energy corresponds to the energy gap between HOMO and LUMO [6]. The observed oxidation potential shift in going from monomeric Chl *a* to its aggregate (probably a dimer) in vitro (130 mV) is smaller than that in vivo (ca. 400 mV) for P700, known to be a Chl *a*/*a*′ heterodimer. This marked difference in the redox potential shift should be due to steric configurations of the dimers in vivo and in vitro, and/or to such chemical influences on P700 as electrostatic interactions and hydrogen bonding from amino acid residues of the protein subunits surrounding P700 [5,20]. Use of

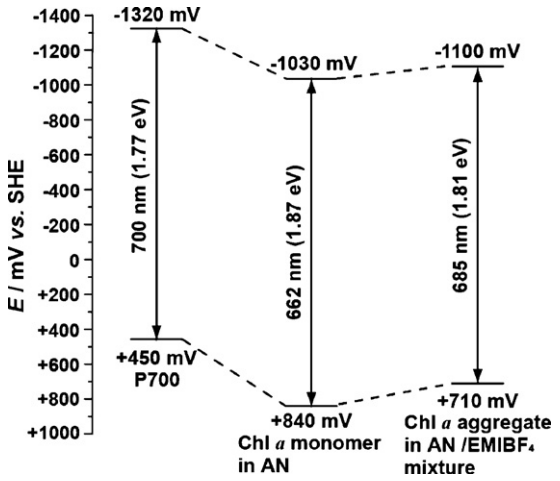

Fig. 6. Redox potential diagram for the Chl *a* monomer, Chl *a* aggregate (probably a Chl *a* dimer) in AN/$EMIBF_4$, and P700 (Chl *a*/*a*′ heterodimer) in PS I.

other ionic liquids with properties, especially acidity/basicity and polarity, different from those of $EMIBF_4$ may yield redox potential shifts to a different degree upon aggregation of Chl *a*. Further examination of the relationship between the properties of ionic liquids and spectroscopic/electrochemical properties of Chl *a* aggregates will yield useful information on the redox potential tuning.

In sharp contrast to P700 possessing a very negative potential as compared to monomeric Chl *a*, PS II of oxygenic photosynthetic organisms generates a strong oxidative power for oxidation of water. The PS II primary electron donor P680, found to be a loose dimer of Chl *a* by crystallography [21], is considered to be the source of the oxidative power. However, the oxidation redox potential of P680 has never been experimentally determined, and hence the chemical entity generating the oxidative power is still controversial. From thermodynamic and kinetic considerations, the redox potential has been estimated to be around +1.2 V *vs.* SHE [22]. Because dimerization of an organic molecule in principle leads to a negative shift of the oxidation potential, as has been verified experimentally in the present work, "the P680 hypothesis" is still enigmatic for the molecular mechanism within PS II.

Acknowledgment

This work was supported in part by a Grant-in-Aid for Scientific Research (C) (No. 19614003) from the Japan Society for the Promotion of Science (JSPS) and a global COE program for "Chemistry Innovation through Cooperation of Science and Engineering" from the Ministry of Education, Culture, Sports, Science and Technology (MEXT) of the Japanese Government.

References

[1] H. Scheer, in: B. Grimm, R.J. Porra, W. Rüdiger, H. Scheer (Eds.), Chlorophylls and Bacteriochlorophylls, Springer, Netherland, 2006, pp. 1–26.
[2] P. Jordan, P. Fromme, H.T. Witt, O. Klukas, W. Saengerand, N. Krauß, Nature 411 (2001) 909–917.
[3] A. Nakamura, M. Akai, E. Yoshida, T. Taki, T. Watanabe, Eur. J. Biochem. 270 (2003) 2446–2458.
[4] B. Ke, Photosynthesis: Photochemistry and Photobiophysics, Kluwer Academic Publishers, 2001.
[5] A. Nakamura, T. Suzawa, Y. Kato, T. Watanabe, FEBS Lett. 579 (2005) 2273–2276.
[6] T. Watanabe, M. Kobayashi, in: H. Scheer (Ed.), Chlorophylls, CRC Press, Boca Raton, FL, 1991, pp. 285–315.
[7] A. Scherz, V. Rosenbach-Belkin, J.R.E. Fisher, in: H. Scheer (Ed.), Chlorophylls, CRC Press, Boca Raton, FL, 1991, pp. 237–268.
[8] A. Agostiano, M. Caselli, M.D. Monica, A.J. Gotch, F.K. Fong, Biochim. Biophys. Acta 936 (1988) 171–178.
[9] A. Agostiano, K.A. Butcher, M.S. Showell, A.J. Gotch, Chem. Phys. Lett. 137 (1987) 37–41.

[10] H. Furukawa, T. Oba, H. Tamiaki, T. Watanabe, J. Phys. Chem. B 103 (7398–7405) (1999).
[11] T. Oba, M. Mimuro, Z.Y. Wang, T. Nozawa, S. Yoshida, T. Watanabe, J. Phys. Chem. B 101 (1997) 3261–3268.
[12] M. Fujiwara, M. Tasumi, J. Phys. Chem. 90 (1986) 250–255.
[13] J.J. Katz, G.L. Gloss, F.C. Pennington, M.R. Thomas, H.H. Strain, J. Am. Chem. Soc. 85 (1963) 3801–3809.
[14] G.L. Closs, J.J. Katz, F.C. Penningston, M.R. Thomas, H.H. Strain, J. Am. Chem. Soc. 85 (1963) 3809–3821.
[15] F.K. Fong, M. Kusunoki, L. Galloway, T.G. Matthews, F.E. Lytle, A.J. Hoff, F.A. Brinkman, J. Am. Chem. Soc. 104 (1982) 2759–2767.
[16] A.J. Bard, L.R. Faulkner, Electrochemical Methods, Fundamentals and Applications, 2nd ed., Wiley, New York, 2001.
[17] H. Weingärtner, Angew. Chem. Int. Ed. 47 (2008) 654–670.
[18] T. Watanabe, A. Hongu, K. Honda, M. Nakazato, M. Konno, S. Saitoh, Anal. Chem. 56 (1984) 251.
[19] M. Kobayashi, S. Ohashi, K. Iwamoto, Y. Shiraiwa, Y. Kato, T. Watanabe, Biochim. Biophys. Acta 1767 (2007) 596–602.
[20] H. Witt, E. Schlodder, C. Teutloff, J. Niklas, E. Bordignon, D. Carbonera, S. Kohler, A. Labahn, W. Lubitz, Biochemistry 41 (2002) 8557–8569.
[21] B. Loll, J. Kern, W. Saenger, A. Zouni, J. Biesiadka1, Nature 438 (2005) 1040–1044.
[22] F. Rappaport, M.G. Kuras, P.J. Nixon, B.A. Diner, J. Lavergne, Biochemistry 41 (2002) 8518–8527.